Supporting Information

Kalayil et al. 10.1073/pnas.1309071110

SI Methods

Expression and Purification. Expression and purification of PmCaiT have been described previously (1). Briefly, *Escherichia coli* BL21 (DE3) pLysS cells were transformed with pET-15b plasmids carrying CaiT from *Proteus mirabilis*. The transformed cells were grown in 2*Yeast extract and Tryptone medium, induced with 0.5 mM IPTG (Isopropyl β-D-1-thiogalactopyranoside) at an OD of 0.6–0.8 at 30 °C and harvested after 4 h. The cells were lysed using a microfluidizer. Cell debris was removed by low-speed centrifugation (10,000 × *g*, 4 °C, 30 min) followed by high-speed centrifugation (125,000 × *g*, 4 °C, 1:30 h) to obtain the membrane fraction. The membranes were homogenized in 25 mM Hepes at pH 7.5, 50 mM NaCl, 20% (vol/vol) glycerol, and 2 mM TCEP (*tris*(2-carboxyethyl)phosphine), flash-frozen, and stored at −80 °C until further use. For crystallization, the membranes were solubilized overnight at 4 °C with 2% (wt/vol) cymal-5 (5-Cyclohexyl-1-Pentyl-β-D-Maltoside), followed by high-speed centrifugation (125,000 × *g*, 4 °C, 1:30 h) to remove detergent-insoluble material. For transport assays and fluorescence binding studies, the membranes were solubilized using 2% (wt/vol) DDM *n*-Dodecyl β-D-maltoside for 2 h at 4 °C. The supernatant was loaded onto a Ni^{2+}-chelating Sepharose column (Amersham), and the protein was eluted using 25 mM Hepes at pH 7.5, 50 mM NaCl, 1 mM TCEP, 0.2% cymal-5/0.05% DDM, and 200 mM Imidazole. The buffer was exchanged on a PD-10 Sephadex column (GE Healthcare) to 25 mM Hepes, 25–50 mM NaCl, 1 mM TCEP, and 0.2% cymal-5 for crystallization and 50 mM Tris, 25–30 mM KCl, 1 mM TCEP, and 0.05% DDM prepared with low-sodium water for transport assays and binding studies. For crystallization, the purified protein was concentrated to 3–5 mg/mL (Vivaspin 100 kDa, Sartorius). All mutant constructs of PmCaiT were generated using the QuikChange Site Directed Mutagenesis kit (Stratagene), according to the manufacturer's instructions. The mutant proteins were purified by the same protocol as for wild-type.

R262E Crystallization and Structure Determination. The purified protein solution was clarified by centrifugation (100,000 × *g*, 4 °C, 30 min) before crystallization. Crystals were grown at 4 °C by vapor diffusion in hanging drops of 2 μL protein solution and 1 μL reservoir buffer [50 mM Ca^{2+}-acetate at pH 4.5–5.5, 0–200 mM NaCl, 19–30% (vol/vol) PEG400]. Crystals appeared after 2–3 d and were frozen directly in liquid nitrogen with 35% (vol/vol) PEG400 as a cryoprotectant. The crystals diffracted isotropically to a resolution of 3.3 Å and belonged to the space group H3, with one molecule in the asymmetric unit. Data were processed using the XDS package (2), and the structure was solved by molecular replacement with wild-type PmCaiT (2WSW) in PHASER (3). The structure was refined with iterative rounds of manual rebuilding in COOT (4) and maximum-likelihood energy minimization and isotropic B-factor refinement in PHENIX (5). Superpositions of various crystal structures were performed on the DaliLite Server (6) or using Secondary-structure matching (SSM) superposition in COOT. All structure figures were generated with Pymol (7).

Reconstitution and Transport Assay. The purified protein was reconstituted into liposomes of *E. coli* polar lipid (Avanti), as described previously (1). Transport assays were performed as described earlier (1, 8). Briefly, proteoliposomes were preloaded with 50 mM Tris at pH 7.5, 1 mM TCEP, and 10 mM γ-butyrobetaine in two freeze–thaw cycles. After the second freeze–thaw cycle, the proteoliposomes were extruded 15 times through a 400-nm membrane filter (Avestin). The extraliposomal substrate was removed by ultracentrifugation (100,000 × *g*, 20 °C, 30 min), and proteoliposomes used for transport measurements were washed with buffer (50 mM Tris at pH 7.5, 1 mM TCEP). Substrate exchange was measured by recording the uptake of L-[*N*-methyl ^{14}C] carnitine hydrochloride (^{14}C-L-carnitine, Perkin-Elmer) into proteoliposomes. Substrate uptake was initiated by 1-μL aliquots of the proteoliposome suspension diluted into 200 μL reaction buffer (50 mM Tris at pH 7.5, 1 mM TCEP) with the concentration of ^{14}C-L-carnitine (2.5 μCi/mL) kept at 40 μM. In addition, 50 mM NaCl was always included in the reaction buffer for Na^+-dependent uptake activity measurements performed with the R262 mutants. For membrane potential measurements, the proteoliposomes also were preloaded with 50 mM KCl, and the reaction buffer was supplemented with 1 μM valinomycin and 50 mM NaCl. For transport kinectics measurements, the concentration of [^{14}C]-L-carnitine was varied from 0.3 to 60 μM. At various times, reaction was stopped by filtering aliquots of the reaction on a Millipore membrane filter (0.22 μm), followed by washing with 3.5 mL of ice-cold Tris buffer (25 mM at pH 7.5). [^{14}C]-L-carnitine uptake was determined with a TRI-CARB 1500 scintillation counter (Canberra-Packard).

Fluorescence Binding Assay. Binding of L-carnitine was measured by tryptophan fluorescence, as described previously (1, 8), with proteoliposomes diluted to 10 μM, in 50 mM Tris at pH 7.5 and 1 mM TCEP with or without 50 mM NaCl, as indicated. The L-carnitine concentration was increased from 0.6 to 175 mM. Data were fitted, and apparent K_d values were obtained using GraphPadPrism.

Homology Modeling. CaiT from *P. mirabilis* was modeled using BetP in the closed [Protein Data Bank (PDB) code 4AIN, chain A] and outward-open (PDB code 4DOJ, chain B) conformation with Modeler 9.11 (9). Twenty models were generated for each conformation, and the five with lowest energy were further analyzed using MolProbity (10). Of these, the model chosen for further analysis had 93.7% and 90.5% of the residues in Ramachandran-favored regions, for closed and outward open conformations, respectively.

Sequence Alignment. The structures of LeuT type transporters with a high degree of structural similarity to the PmCaiT structure (PDB code 2WSW) were obtained on the Dali server (6). The rmsd of the structures varied from 2.2 to 4.4 Å. A multiple sequence alignment of these proteins was generated from the 3D alignment of protein structures with PDBeFold (SSM), and the resulting alignment was manually checked and corrected (11).

1. Jung H, et al. (2002) CaiT of Escherichia coli, a new transporter catalyzing L-carnitine/gamma -butyrobetaine exchange. *J Biol Chem* 277(42):39251–39258.
2. Kabsch W (1993) Automatic processing of rotation diffraction data from crystals of initially unknown symmetry and cell constants. *J Appl Cryst* 26:795–800.
3. McCoy AJ, et al. (2007) Phaser crystallographic software. *J Appl Cryst* 40(Pt 4): 658–674.
4. Emsley P, Cowtan K (2004) Coot: model-building tools for molecular graphics. *Acta Crystallogr D Biol Crystallogr* 60(Pt 12 Pt 1):2126–2132.
5. Adams PD, et al. (2002) PHENIX: building new software for automated crystallographic structure determination. *Acta Crystallogr D Biol Crystallogr* 58(Pt 11):1948–1954.
6. Holm L, Rosenström P (2010) Dali server: conservation mapping in 3D. *Nucleic Acids Res* 38(Web Server issue):W545-9.
7. Delano WL (2002) *The PyMOL Molecular Graphics System* (DeLano Scientific, San Carlos, CA).
8. Schulze S, Köster S, Geldmacher U, Terwisscha van Scheltinga AC, Kühlbrandt W (2010) Structural basis of Na(+)-independent and cooperative substrate/product antiport in CaiT. *Nature* 467(7312):233–236.

9. Eswar N, Eramian D, Webb B, Shen M-Y, Sali A (2008) Protein structure modeling with MODELLER. *Methods Mol Biol* 426:145–159.
10. Davis IW, Murray LW, Richardson JS, Richardson DC (2004) MOLPROBITY: structure validation and all-atom contact analysis for nucleic acids and their complexes. *Nucleic Acids Res* 32(Web Server issue):W615-9.
11. Krissinel E, Henrick K (2004) Secondary-structure matching (SSM), a new tool for fast protein structure alignment in three dimensions. *Acta Crystallogr D Biol Crystallogr* 60(Pt 12 Pt 1):2256–2268.

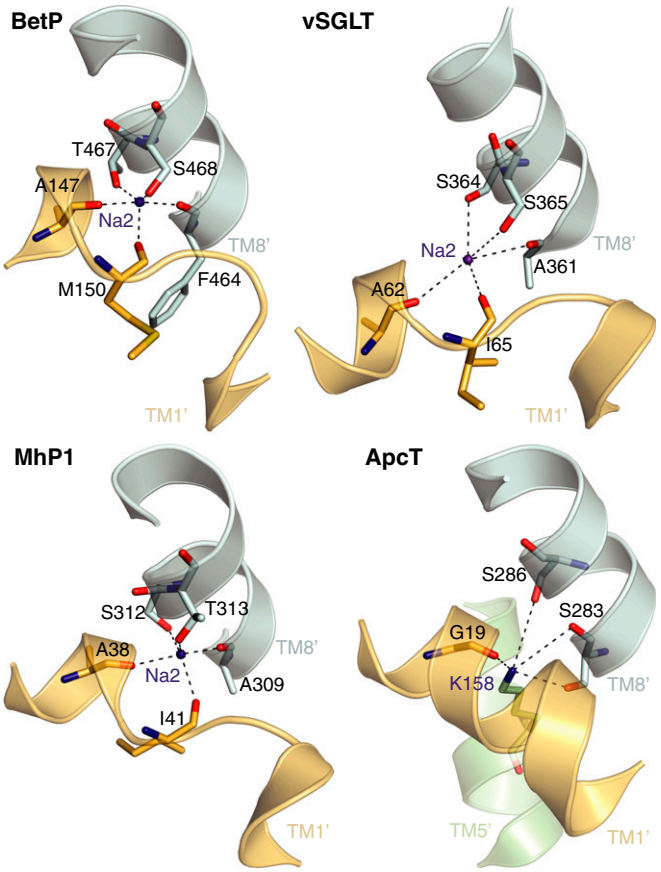

Fig. S1. Comparison of Na2 sites in betaine transporter BetP, Na^+/galactose symporter vSGLT, LeuT-type transporter Mhp1, and H^+-coupled broad-specificity amino acid transporter ApcT. Structures were aligned with wild-type crystal structures of the carnitine transporter CaiT from *Proteus mirabilis* (PmCaiT) at an overall rmsd of 2.7 (BetP), 4.1 (vSGLT), 4.4 (MhP1), and 3.4 Å (ApcT). PDB codes and chains are 4AIN_B for BetP, 3DH4_A for vSGLT, 2JLN_A for MhP1, and 3GIA_A for ApcT. Even though alignments were better for the more similar conformations of BetP (4DOJ_C, rmsd 2.2 Å), vSGLT (2XQ2_A, rmsd 3.8 Å), and MhP1 (2 × 79_A, rmsd 3.6 Å), the Na2-bound conformations were used here for comparison of the Na2 sites. The ApcT structure is rotated by 15° around the *y* axis for a better view of the K158 sidechain.

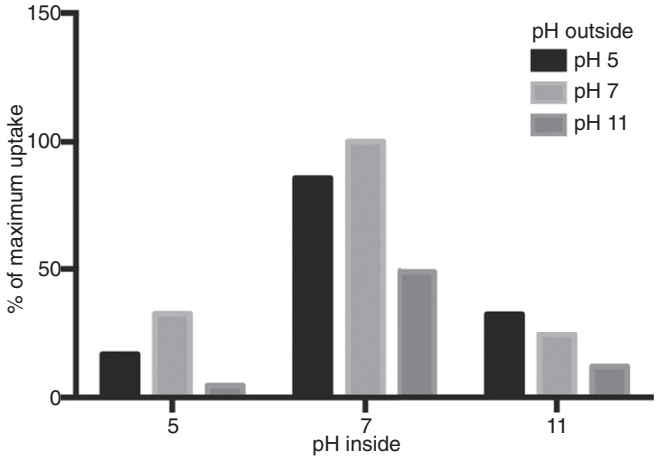

Fig. S2. pH-dependent L-carnitine uptake of wild-type PmCaiT. [^{14}C] L-carnitine uptake activity was measured using proteoliposomes preloaded with 10 mM γ−butyrobetaine. The pH inside the proteoliposomes is denoted on the *x* axis, whereas the pH of the external medium differs for each bar, as indicated. The maximum L-carnitine uptake activity at pH $7_{in}/7_{out}$ is taken as 100%, whereas the others are shown relative to the maximum activity.

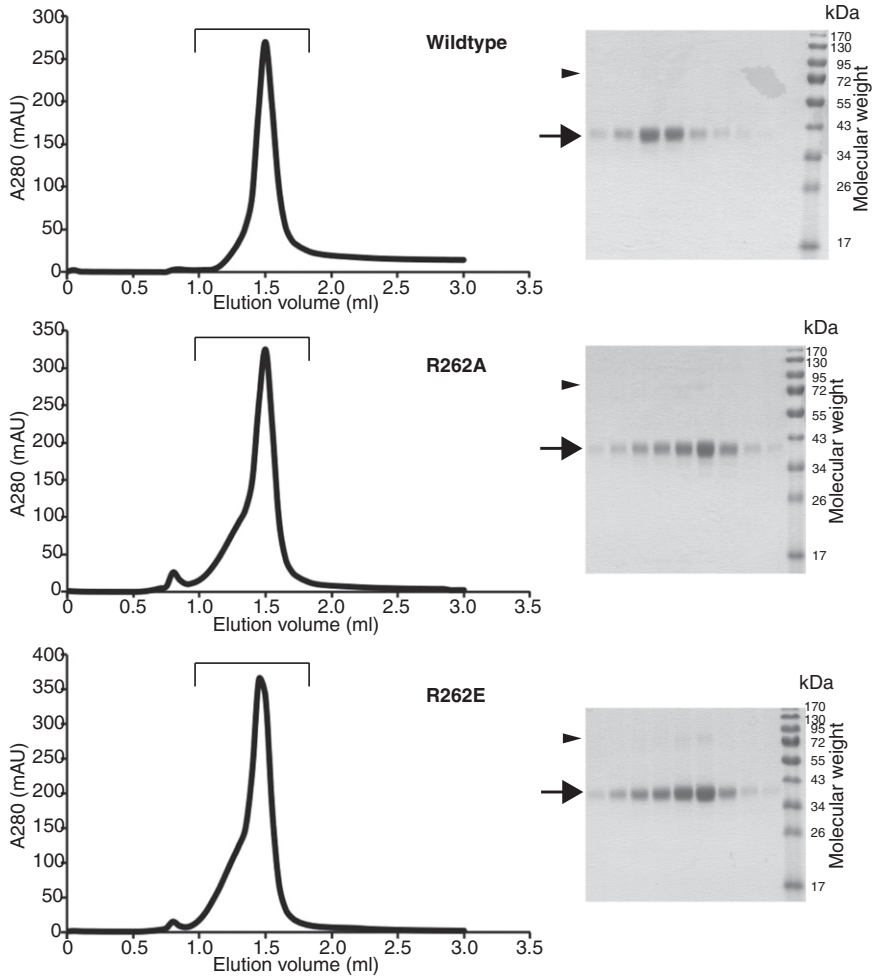

Fig. S3. Analytical size exclusion chromatography (SEC) of PmCaiT wild-type and arginine 262 (R262) mutants. Both the wild-type and the R262 mutants eluted at around 1.5 mL in a Superose-6 (3.2/30) column. The small peak in the void volumes is caused by aggregated protein. The right panel shows the SDS gel of the peak fraction obtained in SEC. The arrow indicates the monomeric protein, and the arrowhead indicates the trimer.

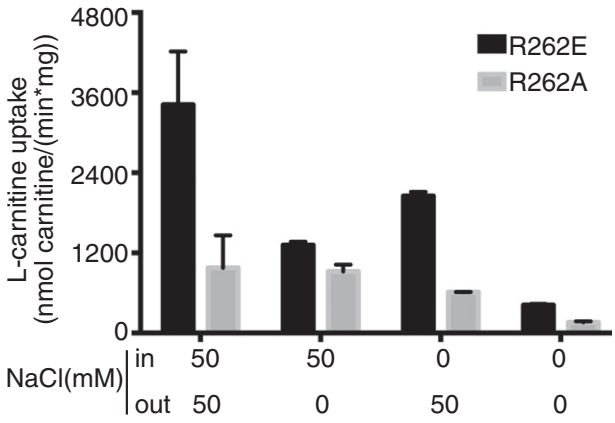

Fig. S4. Na^+-dependent uptake by R262 mutants under different osmotic conditions. Various combinations of NaCl concentrations were used inside and outside the proteoliposomes to ensure the observed effects were not a result of liposome shrinkage.

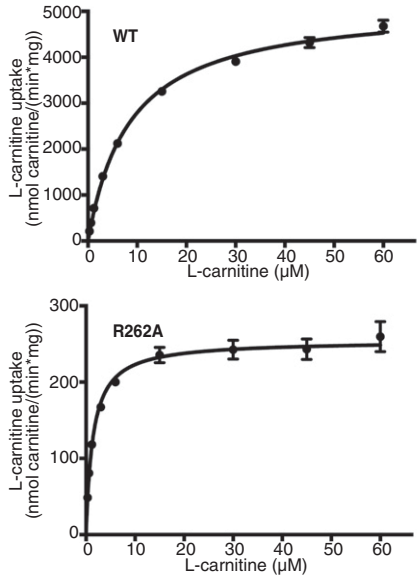

	Km (μM)	Vmax (nmol Car/ (min*mg)	Kcat (sec^{-1})
WT	8.5±0.36	5172±61.8	4.9
R262E	2.4±0.21	660.4±12.8	0.6
R262A	1.4±0.08	254.5±3.07	0.24

Fig. S5. Transport kinetics of PmCaiT wild-type and R262 mutants. The proteoliposomes were preloaded with 10 mM L-carnitine, and L-carnitine counter flow was measured by varying the concentration of [^{14}C] L-carnitine from 0.3 to 60 μM outside the proteoliposomes. The kinetics of mutant proteins were measured in the presence of 50 mM NaCl, both inside and outside the proteoliposomes. All data points are the averages of three independent experiments, and the error bars indicate the SD of the measurements.

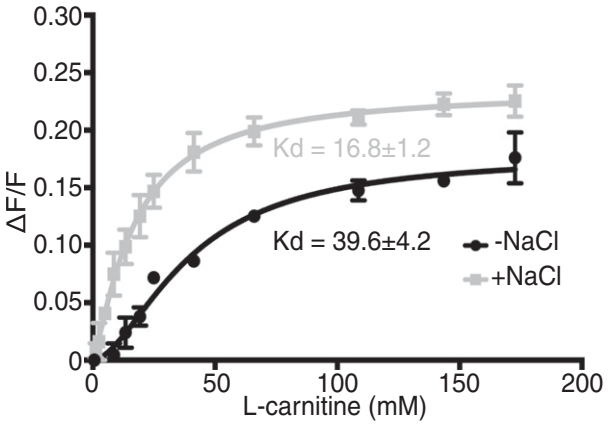

Fig. S6. Tryptophan fluorescence-based substrate-binding experiments with R262A reconstituted into proteoliposomes. The increase in tryptophan fluorescence with rising L-carnitine concentration was monitored in the presence and absence of 50 mM NaCl. The relative increase in fluorescence was plotted using a one-site binding model to obtain the apparent K_d values for substrate binding. All data points are the averages of three independent experiments, and the error bars indicate the SD of the measurements.

```
                                        421
                                        ↓
CaiT   403 LST-ATMWGFFILCFIATVTLINACSYTLAMST 434
BetP   449 GGQ-IMGIIAMILLGTFFITSADSASTVMGTMS 480
GadC   289 TVR-VISALLLLGVLAEIASWIVGPSRGMYVTA 320
MhP1   294 VSIpXAILFQVFVLLATWSTNPAANLLSPAYTL 326
LeuT   336 GGT-FLGFLWFFLLFFAGLTSSIAIMQPMIAFL 367
SGLT   350 -----VKGVVFAALAAAIVSSLASMLNSTATIF 377
```

Fig. S7. Structure-based sequence alignment of TM8′. The alignment of several TM8′ helices from LeuT-type transporters shows conservation of Thr/Ser residues corresponding to T421 in CaiT, which is important for stabilizing the unwound part of TM1′ for substrate binding. Threonine and serine residues are highlighted in orange, and the black arrow shows the highly conserved Thr/Ser involved in Na2 binding.

Table S1. Data collection and refinement statistics

	PmCaiT_R262E
Data collection and scaling	
Wavelength, Å	0.9795
Resolution range, Å	45.90–3.29 (3.55–3.29)
Space group	H3
Cell dimensions	
a, b, c; Å	129.1, 129.1, 160.7
α, β, γ; °	90, 90, 120
Unique reflections	15,128 (3,065)
Multiplicity	5.4 (5.5)
Completeness, %	99.5 (97.9)
Mean I/sigma I	5.6 (2.0)
R_{pim}	0.14 (0.97)
CC(1/2)	0.988 (0.216)
Refinement	
Number of reflections	14,980
Protein residues	495
Number of atoms	3,904
Protein	3,893
Ligand (NM2)	10
Water	1
R_{work}	0.2359 (0.2879)
R_{work}	0.2570 (0.3047)
Ramachandran favored, %	93.7
Ramachandran outliers, %	0.4
RMS (bonds)	0.003
RMS (angles)	0.800
Average B-factors	
Protein	53.5
Ligand	74.8
Solvent	16.9

Statistics for the highest-resolution shell are shown in parentheses.